Article

"Electromers" of the Tetramethyleneethane Radical Cation and Their Nonexistence in the Octamethyl Derivative: Interplay of Experiment and Theory

Beat Mller, Thomas Bally, Fabian Gerson, Armin de Meijere, and Malte von Seebach

J. Am. Chem. Soc., **2003**, 125 (45), 13776-13783• DOI: 10.1021/ja037252v • Publication Date (Web): 18 October 2003

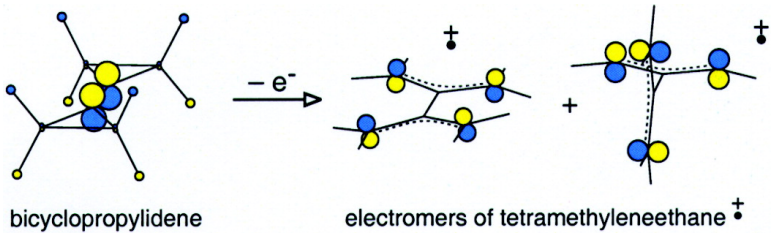

More About This Article

Additional resources and features associated with this article are available within the HTML version:

- Supporting Information
- Links to the 2 articles that cite this article, as of the time of this article download
- Access to high resolution figures
- Links to articles and content related to this article
- Copyright permission to reproduce figures and/or text from this article

View the Full Text HTML

J|A|C|S
ARTICLES
Published on Web 10/18/2003

"Electromers" of the Tetramethyleneethane Radical Cation and Their Nonexistence in the Octamethyl Derivative: Interplay of Experiment and Theory

Beat Müller,[†,||] Thomas Bally,*[,†] Fabian Gerson,[‡] Armin de Meijere,[§] and Malte von Seebach[§]

Contribution from the Department of Chemistry, University of Fribourg, Switzerland; Department of Chemistry, University of Basel, Switzerland; and Institute of Organic Chemistry, Georg-August-University, Göttingen, Germany

Received July 14, 2003; E-mail: thomas.bally@unifr.ch

Abstract: Bicyclopropylidene **1a** and its octamethyl derivative **1b** are subjected to ionization by X-irradiation in solid argon. In accord with previous experiments, this treatment leads to the spontaneous opening of both cyclopropylidene rings, as does ionization of **1b** by γ-irradiation in $CFCl_3$ at 77 K. The resulting tetramethyleneethane (or bisallyl) radical cations $\mathbf{2a}^{+\bullet}$ and $\mathbf{2b}^{+\bullet}$ are distinguished by a broad band in the NIR. In the case of $\mathbf{2a}^{+\bullet}$, wavelength-selective photolyses reveal the presence of *two* interconvertible species with very similar yet distinct spectra. Based on DFT and CASSCF/CASPT2 calculations, these spectra are assigned to two "electromeric" forms of $\mathbf{2a}^{+\bullet}$ which differ in the nature of the singly occupied MO. The NIR bands correspond to charge-resonance transitions between states with fully delocalized spin and charge. Calculations predict that similar electromers should also exist in $\mathbf{2b}^{+\bullet}$ which shows a much weaker NIR band, but no corresponding experimental evidence could be found. On the other hand, the ESR spectrum of $\mathbf{2b}^{+\bullet}$ indicates that, in contrast to $\mathbf{2a}^{+\bullet}$, the spin is largely localized in one of the two allylic moieties in $\mathbf{2b}^{+\bullet}$. Although no theoretical method is presently available that would permit an accurate modeling of the opposing factors favoring localized or delocalized structures in molecules such as $\mathbf{2a}^{+\bullet}$ or $\mathbf{2b}^{+\bullet}$, the observed trends can be satisfactorily rationalized on the basis of semiquantitative considerations. In particular, the important role of vibronic coupling in shaping the potential surfaces for such systems is emphasized.

Introduction

Bicyclopropylidene (**1a**) and its derivatives have proven to be amazingly versatile molecular building blocks.[1] In part, this useful property is due to the unique bonding properties of this compound and its peculiar electronic structure. By virtue of the high s-character of the involved σ hybrid orbitals, the central C=C bond in parent bicyclopropylidene, **1a**, is among the shortest known.[2] Consequently, the oxidation potential is higher than that of other tetraalkylethenes (it is more typical of a dialkylethene), but it still makes **1a** a facile target for electrophiles and cycloaddends.

In 1989, Gerson et al. communicated that ionization of **1a** in a CF_3CCl_3 matrix by γ-irradiation at 77 K resulted in a spontaneous opening of both three-membered rings to yield the radical cation of tetramethyleneethane or 2,2′-biallyl, $\mathbf{2a}^{+\bullet}$.[3] Six years later, the same group reported that, in $CFCl_3$ and $CF_2ClCFCl_2$ matrices, the parent radical cation $\mathbf{1a}^{+\bullet}$ persists up to ca. 100 K.[4] In the former medium, ring opening to $\mathbf{2a}^{+\bullet}$ sets in at this temperature, whereas, in the latter matrix, proton abstraction to yield an allylic radical takes precedence. In no case was the intermediate product of single ring opening detected.

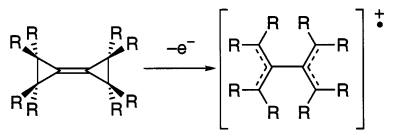

1 **2**$^{+\bullet}$

1a, **2a** : R=H
1b, **2b** : R=CH_3

We have now reinvestigated this reaction in Ar matrices by optical and infrared spectroscopy and surprisingly found that $\mathbf{2a}^{+\bullet}$ exists in two forms, with very similar optical and indistinguishable ESR spectra, which can be reversibly interconverted by selective photolyses. Calculations indicate that the two forms correspond to "electromers", that is, isomers that do not differ much by their bond lengths and angles, but they do rather by their orbital occupancy.

The present study includes also octamethylbicyclopropylidene, **1b**, which had in the meantime become available.[5] In

[†] University of Fribourg.
[‡] University of Basel.
[§] Georg-August-University.
[||] Present address: BUWAL, 3003 Bern, Switzerland.

(1) De Meijere, A.; Kozkoushkov, S. I. *Eur. J. Org. Chem.* **2000**, 3809.
(2) Traetteberg, M.; Arndt, S.; Peters, E. M.; de Meijere, A. *J. Mol. Struct.* **1984**, *118*, 333.
(3) Gerson, F.; de Meijere, A.; Qin, X.-Z. *J. Am. Chem. Soc.* **1989**, *111*, 1135.
(4) Gerson, F.; Schmidlin, R.; de Meijere, A.; Späth, T. *J. Am. Chem. Soc.* **1995**, *117*, 8431.

10.1021/ja037252v CCC: $25.00

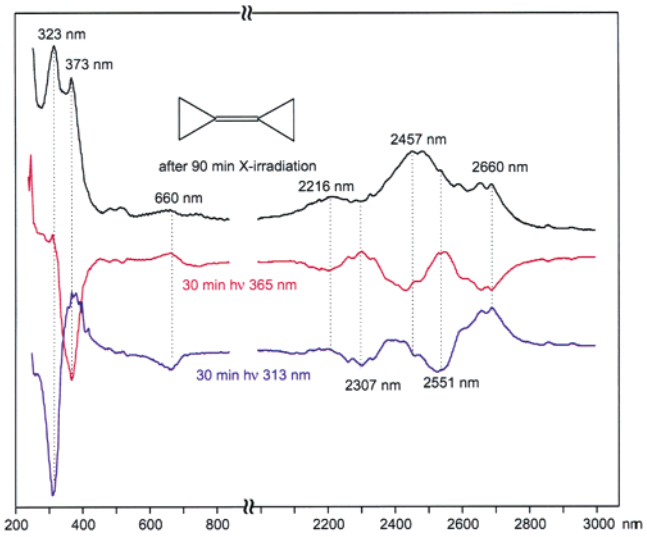

Figure 1. Difference spectra for the ionization of **1a** in Ar at 10 K by X-irradiation (black trace), for the subsequent irradiation at 365 nm (red trace), and finally for the irradiation at 313 nm (blue trace).

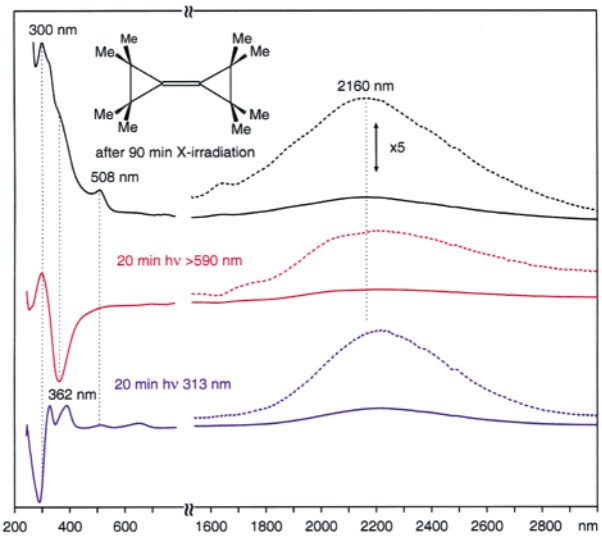

Figure 2. Difference spectra for the ionization of **1b** in Ar at 10 K by X-irradiation (black trace), for the subsequent irradiation at >590 nm (red trace), and finally for the irradiation at 313 nm (blue trace). The dashed lines are expanded 5 times relative to the full lines.

the corresponding bisallylic radical cation, $\mathbf{2b}^{+\bullet}$, no evidence for multiple "electromers" was found. Based on theoretical evidence, we ascribe this finding to a localization of spin and charge in $\mathbf{2b}^{+\bullet}$. Finally, we complemented our study by a computational exploration of the potential surface for the double ring opening of $\mathbf{1a}^{+\bullet}$ and $\mathbf{1b}^{+\bullet}$ to $\mathbf{2a}^{+\bullet}$ and $\mathbf{2b}^{+\bullet}$, respectively. These calculations revealed some interesting features that will be interpreted in terms of vibronic coupling effects. They predict that the reaction occurs stepwise, albeit nearly activationless for the second ring opening.

Experimental Results

1. Optical Spectra. Ionization of **1a** by X-irradiation in Ar at 10 K resulted in no noticeable color change. The electronic absorption (EA) spectrum of a sample treated in this way (Figure 1) reveals the reason: next to two sharp bands in the UV region and an intense system of bands in the near-infrared (NIR) region, the spectrum shows only very weak features in the visible range (and none between 800 and 2000 nm). Irradiation of this sample at 365 nm led to the selective bleaching of the UV band peaking at 373 nm and a part of the NIR band system (red difference spectrum). Moving to 313 nm caused the disappearance of the 323 nm UV band, while the NIR difference spectrum (blue line) showed a mirror-image type relationship to that obtained before on 365 nm irradiation, indicating a partial reconstitution of the species that had been previously bleached.

In Figure 2, the result of a similar experiment with the octamethyl derivative **1b** is shown. After ionization, some similar features appeared in the optical spectrum, but the NIR band was broader and much weaker than in the case of ionized **1a**. Furthermore bleaching at different wavelengths (of which two are shown in Figure 2) did not result in a reversible interconversion but in a continuous growth of the weak NIR band that was accompanied by a weak red-shift. The interconversion observed in the UV on >590 nm irradiation seems to indicate that a precursor absorbing at 362 nm is converted into the radical cation with the broad NIR band (which is probably associated with the 300 nm UV absorption). The changes on 313 nm photolysis are difficult to interpret. They are presumably due to the formation of a secondary product that absorbs in the UV and masks the changes which, in that spectral region, are associated with the formation of the species responsible for the NIR band.

We also attempted to monitor the conversions illustrated in Figures 1 and 2 by IR spectroscopy. Unfortunately, the changes on ionization and subsequent photolysis proved to be too weak to be diagnostically useful, as it is sometimes the case with hydrocarbons that have weak IR absorptions to begin with. The observed IR difference spectra are reproduced, along with those calculated for the two forms of $\mathbf{2a}^{+\bullet}$ in the Supporting Information for future reference.

2. ESR Spectra. The ESR spectra obtained by ionization of **1a** in different Freon matrices were presented and discussed in the previous papers to which the reader is referred.[3,4] The ESR spectrum of an **1b** ionized by γ-irradiation in $CFCl_3$, shown in Figure 3, exhibits 13 hyperfine components spaced by 1.12 ± 0.05 mT due to 12 equivalent or nearly equivalent protons in four methyl groups. Minor hyperfine splittings by the 12 protons

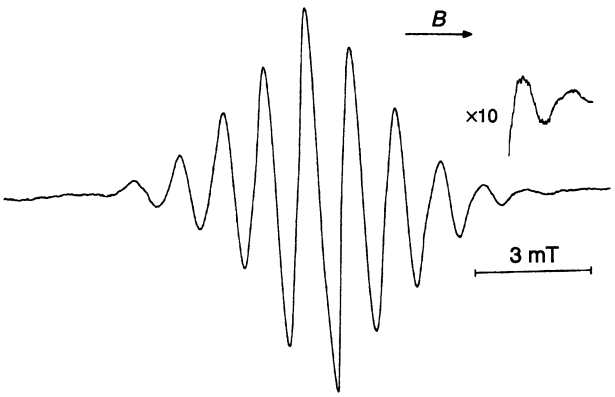

Figure 3. ESR spectrum of **1b** upon ionization by γ-irradiation at 77 K in $CFCl_3$. To optimize the resolution, the spectrum was recorded at 140 K, but the general features of the spectrum did not change between 77 and 140 K.

(5) De Meijere, A.; Seebach, M. v.; Zöllner, S.; Kozhushkov, S. I.; Belov, V. N.; Boese, R.; Haumann, T.; Benet-Buchholz, J.; Yufit, D. S.; Howard, J. A. K. *Chem.—Eur. J.* **2001**, *7*, 4021.

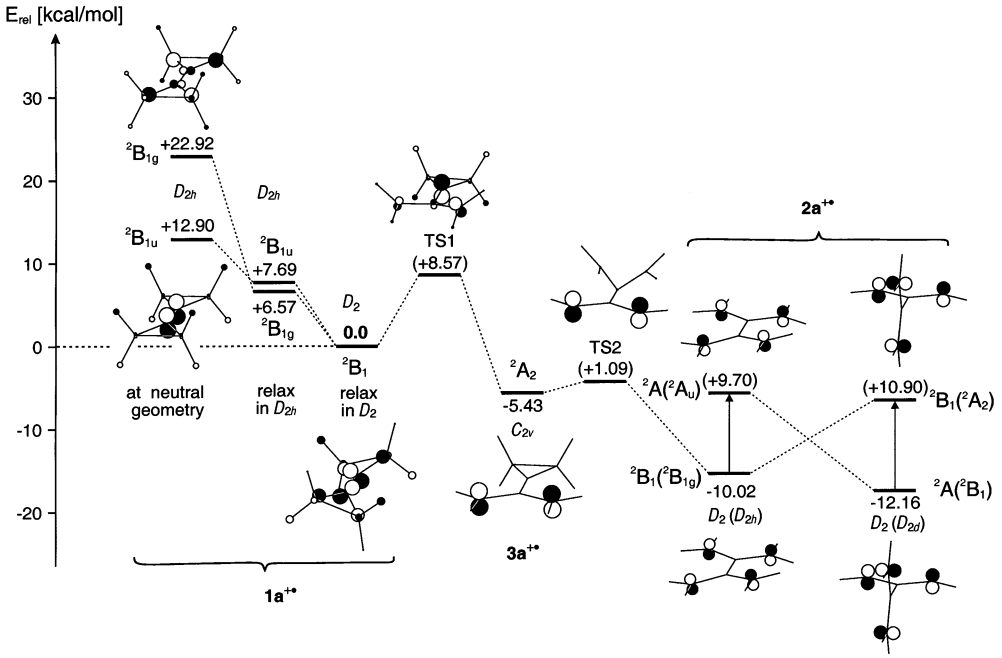

Figure 4. Schematic representation of the potential surface for the ring opening of ionized **1a** (discussion see text). The MO pictures denote the singly occupied MO (SOMO) in the different states. Numbers in parentheses denote activation or vertical excitation energies. In **2a**$^{+\bullet}$, the state symmetries are given with regard to the D_2 point group to facilitate comparison and in the higher symmetries (D_{2h} or D_{2d}, respectively, indicated in parentheses).

Table 1. B3LYP/6-31G* Geometries of **1a**, **1a**$^{+\bullet}$, **2a**$^{+\bullet}$, and **3a**$^{+\bullet}$

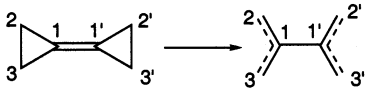

species	symmetry	C_1–$C_{1'}$[a]	C_1–C_2[a]	C_2–C_3[a]	ω[b]
1a (exptl)[c]	D_{2h}	1.314	1.468	1.554	0°
1a (calcd)	D_{2h}	1.311	1.471	1.539	0°
1a$^{+\bullet}$ ($^2B_{1u}$, π)	D_{2h}	1.393	1.451	1.539	0°
1a$^{+\bullet}$ ($^2B_{1g}$, σ)	D_{2h}	1.263	1.553	1.467	0°
1a$^{+\bullet}$ ($^2B_1$, σ/π)	D_2	1.316	1.497	1.499	37.3°
3a$^{+\bullet}$ ($^2A_2$, π)	C_{2v}	1.406	1.448	1.537	0°
			1.416	2.534	
2a$^{+\bullet}$ ($^2B_1$, π)	D_2	1.502	1.389	2.375	10.3°
2a$^{+\bullet}$ (^2A, π)	$D_{2(d)}$	1.500	1.386	2.415	90°

[a] Bond length in Å. [b] Dihedral angle 2−1−1′−2′. [c] Electron diffraction.[2]

of the remaining four methyl groups, as well as possible small deviations for particular methyl groups from the observed major coupling constant of 1.12 mT, are masked by the large width of the 13 components (peak-to-peak distance of 0.55 mT). The values of both of these minor splittings and of possible deviations from 1.12 mT mentioned above are estimated as smaller than 0.2 mT.

Computational Results and Discussion

1. Parent System (1a). Figure 4 sums up the results of DFT calculations of the potential energy surface for the ring opening of **1a**$^{+\bullet}$, while important geometric parameters are detailed in Table 1. Some interesting features emerge from these data.

First, Gerson et al. had already expressed their surprise that the central bond length in **1a** hardly changes on ionization, despite the fact that an electron is removed from a π-MO and that this removal leads to a twisting of nearly 40°. To account for these structural features, one must recall that radical cations often have very close-lying electronic states which are prone to undergo strong vibronic coupling.[6] In the case of **1a**, vertical ionization at the neutral geometry leads to two states spaced by only 0.7 eV,[7] of which the lower one ($^2B_{1u}$) is attained by ionization from the π-HOMO and the upper one ($^2B_{1g}$) by ionization from the antibonding combination of cyclopropyl Walsh MOs depicted on the leftmost side of Figure 4. Relaxation of these two states in their native D_{2h} symmetry results in a pronounced stabilization. The two states become then nearly degenerate in energy, although their geometries differ significantly (cf. Table 1): whereas ionization from the π-HOMO leads to the expected lengthening of the C═C bond, ionization from the b_{1g} MO (which is C_1—$C_{1'}$ antibonding) leads to a significant *shortening* of this bond. However, a vibrational analysis shows that neither of these two geometries represent potential energy minima but both stationary points have negative curvatures along the twisting coordinate.[8]

According to the rules that govern vibronic coupling,[9,10] deformations along coordinates of a_u symmetry ($= b_{1g} \times b_{1u}$) are required to permit interaction of $^2B_{1g}$ and $^2B_{1u}$ states (which both have B_1 symmetry in the resulting D_2 point group). Torsion around the central bond represents such a deformation, and it is, therefore, not surprising that full relaxation of **1a**$^{+\bullet}$ leads to a geometry in which the two cyclopropylidene rings are twisted relative to one another by about 40°. This change is similar to that in ionized parent ethene which is, however, less twisted and has a smaller barrier to planarization.[11] As expected, the twisting in **1a**$^{+\bullet}$ allows the π and the Walsh MO to mix, and, consequently, the two p-AOs on the central C_1—$C_{1'}$ bond end up being nearly orthogonal (cf. Figure 4). The opposing

(6) Williams, F. *Radiat. Phys. Chem.* **2003**, *67*, 211.
(7) Gleiter, R.; Haider, R.; Conia, J.-M.; Barnier, J.-P.; de Meijere, A.; Weber, W. *J. Chem. Soc., Chem. Commun.* **1979**, 130.
(8) The $^2B_{1g}$ state is a saddle point, and the $^2B_{1u}$ state has two directions of negative curvature, one of them corresponding to the twisting deformation.
(9) Köppel, H.; Cederbaum, L. S.; Domcke, W.; Shaik, S. S. *Angew. Chem., Int. Ed. Engl.* **1983**, *22*, 210.
(10) Bersuker, I. B. *The Jahn−Teller Effect and Vibronic Interactions in Modern Chemistry*; Plenum Press: New York, 1984; pp 61−72.
(11) Abrams, M. L.; Valeev, E. F.; Sherill, C. D.; Crawford, T. D. *J. Phys. Chem. A* **2002**, *106*, 2671.

Table 2. Excited States of $\mathbf{2}^{+\bullet}$ at the Planar (D_{2h}) and Perpendicular (D_{2d}) Geometries by CASSCF/CASPT2 Calculations

	state	eV	nm	*f*
planar (D_{2h})	1^2B_{1g}	(0)		
	1^2A_u	0.49	2555	0.049
	1^2B_{3u}	2.37	524	0.009
	2^2B_{3u}	3.14	395	0.017
	3^2B_{3u}	5.10	243	0.339
perpendicular (D_{2d})	1^2A	(0)		
	1^2B_1	0.63	1978	0.066
	1^2E	2.61	475	0.002
	2^2E	3.59	346	0.002
	2^2B_1	4.80	258	0.365

tendencies of the two contributing states with regard to the central bond tend to cancel, and this cancellation apparently results in almost no net change of the C═C bond length on ionization. Similarly, the lengths of the C_1—C_2 and the C_2—C_3 bonds represent averages of those found in the "parent" $^2B_{1g}$ and $^2B_{1u}$ states.

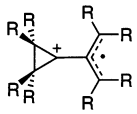

3a: R=H
3b: R=CH_3

The opening of the first cyclopropylidene ring, which leads to the trimethylenemethane-type radical cation, $\mathbf{3a}^{+\bullet}$, is associated with a barrier of ca. 7.9 kcal/mol on an enthalpy scale (i.e., $E_a = 8.1$ kcal/mol at 100 K, the temperature at which opening was observed in $CFCl_3$). With this barrier and $A \approx 2 \times 10^{13}$, the reaction would be too slow to be observed, but it is possible that the reaction is significantly accelerated in a polarizable medium, because the charge is localized essentially in the breaking bond of the transition state, whereas it is fully delocalized in the reactant. According to calculations, the product radical cation, $\mathbf{3a}^{+\bullet}$, does not enjoy a great deal of persistence, because the barrier for the opening of the second ring is less than 1 kcal/mol on a B3LYP enthalpy scale (and it may disappear altogether at higher levels of theory). Thus, it is not surprising that the previous ESR and the current optical experiments have yielded no evidence for the presence of $\mathbf{3a}^{+\bullet}$.

The final product, $\mathbf{2a}^{+\bullet}$, is formed in a state where the two allylic moeties are nearly coplanar (twisted by ca. 10° but with almost no barrier for planarization). As we intended to assign the spectrum obtained after ionization of **1a** to this product, we embarked on excited-state calculations by the CASSF/CASPT2 method. Representative results of these calculations (which for reasons of computational economy were carried out at the planar D_{2h} geometry) are shown in the top part of Table 2. The most prominent absorption of planar $\mathbf{2a}^{+\bullet}$ occurs indeed in the NIR, close to the maximum absorption in the experimental spectrum, whereas no further absorptions of significant intensity are predicted up to the UV region, barring a weak transition at 524 nm which may be assigned to the hump at 660 nm. The observed band at 373 nm corresponds probably to that predicted at 395 nm by CASPT2, whereas the intense transition predicted at 243 nm may be blocked by absorptions of neutral **1a** which is always present in large excess in the matrix.

The NIR transition corresponds largely to promotion of an electron from the b_{1g} SOMO (b_1 in D_2) to the a_u LUMO (a in D_2), that is, from the positive to the negative combination of the nonbonding allylic MOs (NBMOs, cf. Figure 4). Thus, it represents a "charge-resonance" (CR) transition[12] such as they occur typically in the NIR spectra of dimer radical cations.[13] Usually, such CR transitions show no vibrational fine structure, but in the present case, a progression of ca. 400 cm^{-1} can be discerned in the NIR band. By means of a separate DFT calculation on the ^2A_u state (at the geometry of the $^2B_{1g}$ ground state), this CR excitation is predicted to occur at 0.45 eV, in excellent accord with the above CASPT2 result (on twisting by 10.3°, it drops to 0.42 eV). Upon optimization of this excited state in D_2 symmetry, it collapses to a perpendicular structure which profits from *spiroconjugation* between the two allylic moieties. This perpendicular structure (of which the electronic states are labeled on the rightmost side of Figure 4 in D_2 symmetry for consistency) also has a CR transition in the NIR corresponding here to electron promotion from the spiro-bonding to spiro-antibonding combination of allyl NBMOs; no further transitions of significant intensity are predicted down to 258 nm (see lower part of Table 2). Relaxation of the excited state at the perpendicular geometry leads to the ground state of the initially formed (nearly) planar geometry.

The above results account very well for the observation of a reversible photoinduced interconversion between two forms of $\mathbf{2a}^{+\bullet}$ that differ by the nature of the singly occupied MO but have a similar disposition of excited states. Apart from the dihedral angle between the allylic moieties, the geometries of the two states of $\mathbf{2a}^{+\bullet}$ are nearly the same (cf. last two rows of Table 1), yet they are physically distinct entities. One may want to describe this peculiar kind of isomerism by the term "electromers"(which is used in organometallic chemistry to define distinct species that differ mainly by the oxidation state of the metal)[14] or "lumomers" (to highlight the fact that the HOMOs and the LUMOs correlate).[15]

It is noteworthy that the two "electromers" of $\mathbf{2a}^{+\bullet}$ have a very similar distribution of the unpaired electron (the Mulliken spin populations at the termini of the allylic units are identical to within 0.005 electrons in the two states). Hence, the two "electromers" of $\mathbf{2a}^{+\bullet}$ are not expected to give rise to distinguishable ESR spectra, or turned round, the ESR spectra would not show the existence of these "electromers", in contrast to the optical spectra. In addition, the two species possibly undergo rapid *thermal* interconversion on the hyperfine time scale at 100 K if the barrier on the ground-state surface is sufficiently low.

Attempts to calculate that barrier (i.e., to find the transition state for the interconversion on the ground-state surface) run into an interesting problem: an adiabatic crossing from the reactant to the product surface is impossible in D_2 symmetry, because the two states belong to different irreducible representations ($^2B_1$ and ^2A, respectively). Therefore, the reaction is forced

(12) Badger, B.; Brocklehurst, B. *Trans. Faraday Soc.* **1970**, *66*, 2939.
(13) Badger, B.; Brocklehurst, B. *Trans. Faraday Soc.* **1969**, *65*, 2576, 2582, 2588.
(14) Visser, S. P. d.; Ogliaro, F.; Harris, N.; Shaik, S. *J. Am. Chem. Soc.* **2001**, *123*, 3037.
(15) We had previously encountered a case of a bisallylic radical cation, bicyclo-[3.3.0]octa-2.6-diene-4,8-diyl, with a similar CR transition involving the bonding and the antibonding combination of allyl-NBMOs (Bally, T.; Truttmann, L.; Dai, S.; Wang, J. T.; Williams, F. *Chem. Phys. Lett.* **1993**, *212*, 141). However, in that case, the molecular framework did not allow for a relaxation of the excited state to a new ground-state equilibrium structure with the same atomic connectivities but with a distinct electronic structure (instead, this species underwent photoinduced tautomerization).

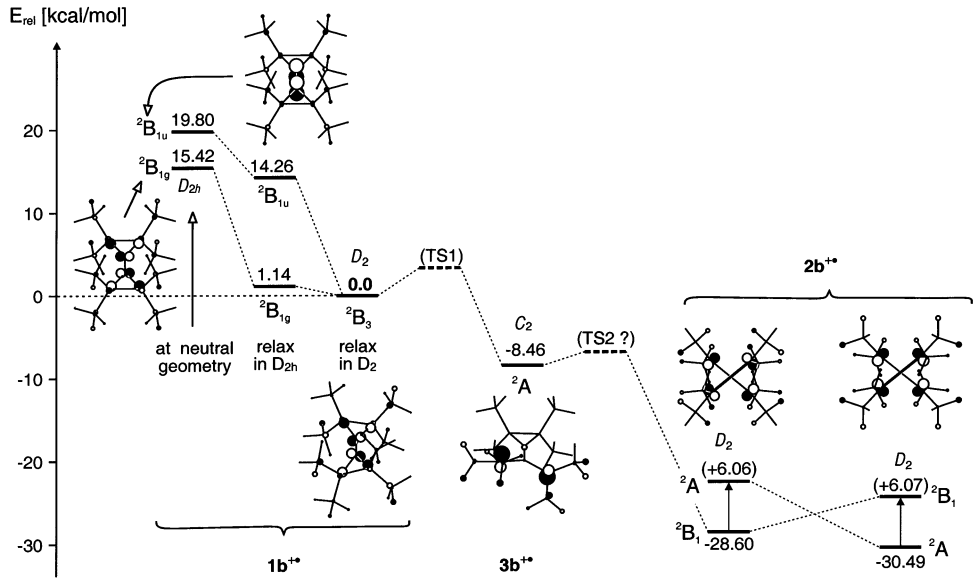

Figure 5. Schematic representation of the potential surface for the ring opening of ionized **1b** (discussion see text). The MO pictures denote the singly occupied MO (SOMO) in the different states. Numbers in parentheses denote vertical excitation energies.

to go through a conical intersection in the D_2 subspace of geometries. However, such conical intersections are invariably surrounded by a "moat"[16] through which the system can pass to *avoid* the conical intersection, and this moat contains a true transition state for the thermal reaction. To find the pertinent point on going from the planar to the perpendicular state of **2a**$^{+\bullet}$, the signs of the p-AOs in one-half of the SOMO must change, but they can only do so by going through zero at some point, which implies a distortion of the wave function from D_2 to C_2 symmetry. Physically, such a distortion is tantamount to a localization of the spin in one of the two allyl moieties (and, formally, the localization of the charge in the opposite one), and this localization will be accompanied by a corresponding geometry change.

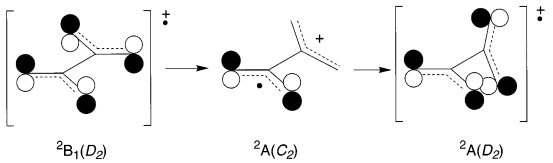

Unfortunately, density functional methods are inherently incapable of modeling correctly such situations due to the incomplete cancellation of the electron self-interaction[17] which leads to an artifactual preference for delocalized over localized states of radical ions.[18,19] The same problem had previously prevented us from finding the transition state for the rotation around the central bond in the radical cation of butadiene.[20] As Hartree−Fock methods do not account for dynamic electron correlation (which is an important contributor to the stability of systems with delocalized electrons), they tend to favor localized over delocalized wave functions in species such as **2a**$^{+\bullet}$, a default that cannot be rectified properly by introducing electron correlation with perturbative methods. Because such wave-function-based methods are also unsuitable for a correct modeling of this process (cf. following section), we decided not to pursue the matter further at that point.

Table 3. B3LYP/6-31G* Geometries of **1b**, **1b**$^{+\bullet}$, **2b**$^{+\bullet}$, and **3b**$^{+\bullet}$[a]

species	symmetry	C_1–C_1[b]	C_1–C_2[b]	C_2–C_3[b]	ω[c]
1b	D_{2h}	1.315	1.481	1.565	0°
1b$^{+\bullet}$ ($^2B_{1u}$, π)	D_{2h}	1.394	1.459	1.570	0°
1b$^{+\bullet}$ ($^2B_{1g}$, σ)	D_{2h}	1.269	1.563	1.498	0°
1b$^{+\bullet}$ ($^2B_1$, σ/π)	D_2	1.290	1.537	1.510	26.9°
3b$^{+\bullet}$ ($^2A_2$, π)	C_2	1.383	1.474	1.552	14.1°
			1.448	2.530	
2b$^{+\bullet}$ ($^2B_1$, π)	D_2	1.531	1.406	2.510	78.1°
2b$^{+\bullet}$ (^2A, π)	D_2	1.516	1.409	2.513	77.4°

[a] For the numbering of carbon atoms, cf. Table 1. [b] Bond length in Å. [c] Dihedral angle 2−1−1′−2′.

2. Octamethyl Derivative 1b. The optical spectra obtained after ionization of **1b** give no indication of an interconversion of different states of the presumed ring-opened cation, **2b**$^{+\bullet}$, and the NIR bands are much weaker in this case than in that of the parent compound **2a**$^{+\bullet}$. Again, calculations proved helpful to rationalize these observations.

Figure 5 and Table 3 summarize the results of calculations analogous to those shown in Figure 4 and Table 1 for the parent compound. Remarkably, the ordering of states in **1b**$^{+\bullet}$ has changed relative to that in **1a**$^{+\bullet}$ in that the state arising by ionization from the cyclopropyl Walsh-MOs is now the *ground state*, even at the geometry of the neutral compound **1b**. As this state profits more from relaxation in D_{2h} than that attained by removal of an electron from the b_{1u} π-MO, the two states are finally separated by over 13 kcal/mol at the respective optimized D_{2h} geometries (and even more so vertically). Consequently, the mixing of states induced by torsion around the central bond in **1b**$^{+\bullet}$ is not quite as strong as in **1a**$^{+\bullet}$, and the features of the lower-lying $^2B_{1g}$ state are expected to prevail at the twisted (D_2) equilibrium geometry of **1b**$^{+\bullet}$. A manifestation of these features is that the length of the central bond in **1b** actually *shrinks* on ionization, while the C_1−C_2 bonds undergo more than twice as much lengthening as in parent in

(16) For example, see: Blancafort, L.; Adam, W.; Gonzalez, D.; Olivucci, M.; Vreven, T.; Robb, M. A. *J. Am. Chem. Soc.* **1999**, *121*, 10583.
(17) Sodupe, M.; Bertran, J.; Rodriguez-Santiago, L.; Baerends, E. J. *J. Phys. Chem. A* **1999**, *103*, 166.
(18) Bally, T.; Sastry, G. N. *J. Phys. Chem. A* **1997**, *101*, 7923.
(19) Bally, T.; Borden, W. T. *Rev. Comput. Chem.* **1999**, *13*, 1.
(20) Sastry, G. N.; Bally, T.; Hrouda, V.; Carsky, P. *J. Am. Chem. Soc.* **1998**, *120*, 9323.

1a$^{+\bullet}$. Due to the repulsion between the eclipsed methyl groups, the C_2-C_3 bonds are generally longer in **1b**$^{+\bullet}$ than in **1a**$^{+\bullet}$.

Unfortunately, because of the many degrees of freedom introduced by the eight methyl groups, we were unable to pin down a saddle point with only a single direction of negative curvature that corresponds to the reaction coordinate for the opening of the first ring in **1b**$^{+\bullet}$. However, several second-order saddle points were located which show a direction of negative curvature matching the expected reaction coordinate (while the other indicated some movement in the methyl groups), and all of those were 4−5 kcal/mol above the D_2 equilibrium structure of **1b**$^{+\bullet}$. Thus, we presume that the activation energy for this process has dropped to about half the value it had in **1a**$^{+\bullet}$; that is, chances of "catching" the primary cation **1b**$^{+\bullet}$ even in a cryogenic experiment are minimal.

The ring-opened species **3b**$^{+\bullet}$ shows similar structural features as its parent counterpart, **3a**$^{+\bullet}$, except that, due to the repulsion between the methyl groups, it is twisted and also rotated about the allylic bonds, a structural change which reduces the symmetry to C_2. However, **3b**$^{+\bullet}$ is again a species that can at most have a very fleeting existence, because it is barely protected from decay to the bisallylic product, **2b**$^{+\bullet}$ (although **3b**$^{+\bullet}$ is a potential energy minimum, all attempts to locate the transition state for the opening of the second ring converged to **2b**$^{+\bullet}$). The activation energy for that process must, therefore, be very small indeed, in accord with the much greater exothermicity of the second ring-opening process in the octamethyl derivative **3b**$^{+\bullet}$ (cf. Figures 4 and 5).

As in the case of **2a**$^{+\bullet}$, the octamethyl derivative **2b**$^{+\bullet}$ exists in the form of two "electromers" which, however, do not even differ much by the dihedral angle between the allylic units in this case, because steric constraints prevent the $^2B_1$ state from attaining the (principally desired) planarity. As a consequence, the distance between the allylic termini increases from 2.95 Å to 3.32 Å in the $^2B_1$ states on going from **2a**$^{+\bullet}$ to **2b**$^{+\bullet}$, which makes the vertical CR excitation energies ($^2B_1 \rightarrow {}^2A$ or vice versa) even lower in **2b**$^{+\bullet}$ than in **2a**$^{+\bullet}$. Thus, one would expect that the corresponding optical transitions occur even further in the IR, the contrary of what was observed (cf. Figures 1 and 2). Conversely, the *intensity* of the SOMO → LUMO transitions is not expected to suffer from methyl substitution, because the shape of the involved MOs does not change appreciably on going from **2a**$^{+\bullet}$ to **2b**$^{+\bullet}$. Nonetheless, the experimental spectra show a pronounced decrease in the intensity of the NIR transition in **2b**$^{+\bullet}$; thus, the latter prediction is also in disagreement with observation. Finally, we recall that (a) the optical spectra of **2b**$^{+\bullet}$ give no indication for the presence of two "electromers" as it is clearly the case in those of **2a**$^{+\bullet}$ and (b) the ESR spectra show substantial coupling to only half of the protons in **2b**$^{+\bullet}$.

All these discrepancies between experiment and theory can be reconciled if spin and charge are assumed to be largely localized in opposite allylic moieties of **2b**$^{+\bullet}$: First, the major hyperfine splitting will be due to only 12 out of 24 protons. Second, the NIR charge-resonance transition will give way to a *charge-transfer* transition between the allylic moieties. The intensity of this transition is expected to be much weaker than that of a CR transition (if the localization of spin and charge is complete, there is almost no overlap between the HOMO and the LUMO and the transition moment will be practically zero)

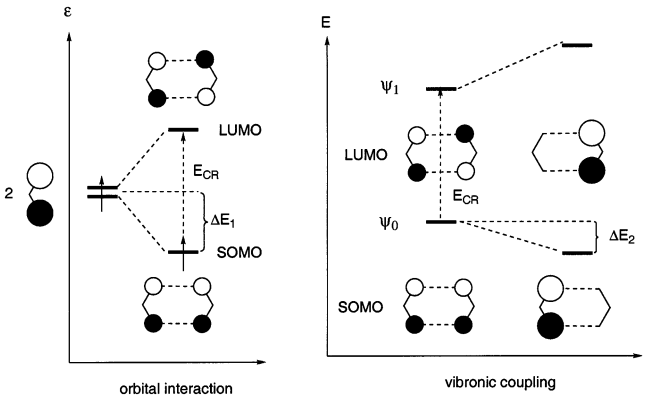

Figure 6. Factors that contribute to the localization/delocalization of spin and charge in bisallylic systems.

and may well be somewhat blue-shifted from the former. Finally, spin and charge localization will lead to a collapse of the two "electromers" to a single species, thus explaining the fact that the optical spectra show only one compound absorbing in the NIR.

However, we recall at this point that a bisallylic species with localized spin and charge is supposed to correspond to the *transition state* for the interconversion of the two delocalized electromers of the tetramethyleneethane radical cations **2**$^{+\bullet}$, the situation which apparently prevails in parent **2a**$^{+\bullet}$. How can octamethyl substitution convert this transition state into a minimum? To answer this question, one must realize that the competition between localized and delocalized states of such bisallylic species involves a subtle interplay of different factors. The operation of two of these factors is schematically illustrated in Figure 6. When two π-systems that together contain an odd number of π-electrons interact (through space or via intervening σ-bonds), this interaction results in a stabilization ΔE_1 that corresponds (in a Hückel approximation) to half the energy of the charge-resonance transition, E_{CR}, in that compound.

On the other hand, the ground state may profit from vibronic coupling with the CR excited state, provided the system lowers its symmetry to a point group in which the two states belong to the same irreducible representation (cf. right-hand side of Figure 6). In the present case, this structural feature corresponds to a localization of the SOMO (i.e., the unpaired electron) and the LUMO in opposite allyl moieties. Of course, such localization entails a loss of the stabilization ΔE_1, but if the lowering of the ground-state energy through vibronic coupling, ΔE_2, outweighs ΔE_1, then localization is eventually favored (it is also conceivable that the system strikes a compromise by undergoing only *partial* localization of the spin, to retain a measure of stabilization through MO interaction). The magnitude of ΔE is proportional to a matrix element $\langle\psi_0|H'|\psi_1\rangle$ which describes the extent of mixing of the ground- and the excited-state wave function upon distortion and is *indirectly* proportional to the energy difference between the two states, in our case E_{CR}.

As noted above, E_{CR} decreases by about 50% on going from **2a**$^{+\bullet}$ to **2b**$^{+\bullet}$ (according to our DFT calculations). Thus, ΔE_1 is expected to decrease by a similar percentage, whereas ΔE_2 will *increase* by about 50%, because E_{CR} appears in the denominator of the expression for ΔE_2. Consequently, methyl substitution in **2**$^{+\bullet}$ may well tip the balance in favor of a localized equilibrium structure, although this structure represents a

transition state in $\mathbf{2a}^{+\bullet}$, and we surmise that this is indeed what is happening.

At this point, the reader may wonder why we did not launch into a computational exploration of this phenomenon to substantiate the above hypothesis. The reason is the same as that invoked above for our failure to find the transition state for the interconversion of the electromers in $\mathbf{2a}^{+\bullet}$: an accurate modeling of the above-described factors requires a correct account for dynamic electron correlation (which favors situations where electrons have more space available to avoid each other, i.e., delocalized structures). Thus, Hartree−Fock SCF methods which do not account for electron correlation invariably predict localized states of $\mathbf{2}^{+\bullet}$ to be considerably more stable than delocalized ones, even in $\mathbf{2a}^{+\bullet}$.[21] Changing a fully localized into a fully delocalized wave function is clearly beyond the capabilities of low-order perturbation theory; hence, the popular MP2 method for reintroducing correlation energy into HF wave functions is bound to fail in this case (and it gives indeed very strange results). Because the otherwise very useful DFT methods, which account very efficiently for correlation energy, overstabilize delocalized states for other reasons,[17] we are currently bereft of any theoretical tool that would allow us to correctly model the potential energy surface of a species the size of $\mathbf{2b}^{+\bullet}$.[22]

Thus, we are restricted to qualitative reasoning and use this method to account for another feature of the ESR experiment described at the outset that still awaits clarification. It is the finding that the observed coupling constant to the 12 protons in $\mathbf{2b}^{+\bullet}$ (1.12 ± 0.05 mT) is too small for a structure in which the spin is fully localized in one of the two allyl moieties. Suitable reference systems are the 1,1,3,3-tetramethylallyl radical where the protons of the methyl groups show hyperfine splittings of 1.42 mT (*exo*) and 1.30 mT (*endo*)[23] or the ring-opened tetramethyloxirane radical cation for which a 12-proton value of 1.51 mT was reported[24] (coupling constants to such methyl protons are generally found to increase on going from neutral to charged radicals[25a]). For the fully delocalized $\mathbf{2b}^{+\bullet}$, B3LYP predicts averaged couplings of +0.61 and +0.93 mT for the protons of the *endo*- and *exo*-methyl groups. Assuming that these couplings would double on full localization of the spin leads to predictions of +1.22 and +1.86 mT or an average of +1.54 mT.[26]

Because the observed major coupling constant of the 12 protons in the four methyl groups of the spin-bearing allyl moiety of $\mathbf{1b}^{+\bullet}$ is about 25% lower than expected for a fully localized structure, the minor coupling constant of the 12 protons in the four methyl groups of the second allyl moiety should correspond to this deficiency; that is, it should be ca. 0.4 mT. The fact that this value is presumably smaller than 0.2 mT and escapes direct observation (see Experimental Results) may be due to a contribution of an opposite sign which is transmitted to the methyl groups of the second moiety from the central carbon atom of the spin-bearing allyl moiety. It is well-known that the corresponding carbon atom in the allyl radical accommodates an appreciable negative π-spin population (−0.18).[25a] A possible difference in the observed coupling constant of the 12 strongly coupled protons which would arise from the *exo*- and *endo*-positions, each of two methyl groups, should also be smaller than 0.2 mT.

Again, we can offer no quantitative theoretical foundation to this proposal, but we can see no principal reason why a system such as $\mathbf{2b}^{+\bullet}$ should necessarily be either fully delocalized or fully localized. Surely, a situation can arise where the different factors that compete in making one or the other situation more favorable hold a balance which can, for example, be slightly shifted by solvation (which favors a structure with localized charge). Solvent-dependent partial localization of the π-spin population was observed for several radical anions containing two equivalent π-moieties and associated with their alkali-metal counterions.[25b]

Finally, having proposed that partial localization of spin and charge may explain the various experimental observations made on $\mathbf{2b}^{+\bullet}$, we turn again to $\mathbf{2a}^{+\bullet}$ and consider the possibility that this radical cation *appears* as a delocalized species, because the spin hops back and forth between the two allyl moieties with a rate that is rapid on the hyperfine time scale at 100 K. Although this possibility cannot rigorously be excluded, several facts speak against such a hypothesis: (a) In Ar at 10 K, $\mathbf{2a}^{+\bullet}$ appears in two similar, yet distinct forms which can readily be assigned in terms of two "electromers". It would be difficult to explain the photochemical interconversions documented in Figure 1 if $\mathbf{2a}^{+\bullet}$ would be a localized species similar to $\mathbf{2b}^{+\bullet}$ where such interconversions do not occur. (b) Because the two species do not interconvert at 12 K in Ar for days, the transition state between them (i.e., the localized state) must lie at least 1 kcal/mol above the higher of the two minima in Ar. It is unlikely that going to $CFCl_3$ results in sufficiently strong differential solvation effects to lower the localized state below the two delocalized electromers. (c) As $\mathbf{2b}^{+\bullet}$ exists as a localized species in $CFCl_3$ at 100 K, the activation barrier for spin hopping is apparently too high to be perceived on the hyperfine time scale. There is no apparent reason why this barrier should be significantly lower in $\mathbf{2a}^{+\bullet}$.

Thus, $\mathbf{2a}^{+\bullet}$ should exist as a fully delocalized species also in $CFCl_3$ at 100 K. What cannot be excluded is that the two electromers equilibrate rapidly under these conditions. Due to the similarity of the predicted ESR spectra for the two electromers, this process is, however, unlikely to manifest itself in a palpable fashion, even if one could lower the temperature to a point where it becomes slow on the hyperfine time scale.

(21) In unrestricted Hartree−Fock (UHF) calculations, the preference for localized states is as much as 12−14 kcal/mol (see Supporting Information), but this peference is, in part, due to an overaccount for spin polarization which comes about by an increased admixture of higher spin states on localizing the unpaired electron in a single allyl moiety (this admixture is manifested by an increase of the expectation value of S^2 by 0.2). In ROHF, the preference for localized states is smaller, but this method is useless in the present context, because it ignores spin polarization and, in addition, shows pronounced symmetry breaking in the localized state. A way out of this impasse would be to use CASSCF (which models spin polarization through an admixture of singly excited states). We did indeed carry out such calculations, but they also invariably resulted in localized structures, in disagreement with experiment for the parent radical cation.

(22) The parent system is small enough that it could possibly be treated by coupled cluster methods, but even those methods would probably find it difficult to strike the right balance between the opposing forces, given the dubious quality of the one-electron wave functions on which they would have to be based in the present case.

(23) Kirwan, J. N.; Roberts, B. P. *J. Chem. Soc., Perkin Trans. 2* **1989**, 539.

(24) Rideout, J.; Symons, M. C. R. *J. Chem. Soc., Faraday Trans. 1* **1986**, *82*, 167.

(25) Gerson, F.; Huber, W. *Electron Spin Resonance of Organic Radicals*; Wiley-VCH: Weinheim, Germany, 2003; (a) Chapter 4.2 and (b) Chapter 6.6.

(26) The difference in the *endo*/*exo* coupling constants predicted by B3LYP is usually too large, but the average value is predicted correctly within <0.1 mT in allylic radicals carrying methyl groups (Müller, B.; Bally, T. Unpublished results).

Conclusions

Ionization of bicyclopropylidene **1a** and its octamethyl derivative **1b** by X-irradiation in solid argon leads to the spontaneous opening of both cyclopropylidene rings as does ionization of **1b** by γ-irradiation in $CFCl_3$ at 77 K. The resulting tetramethyleneethane radical cations $\mathbf{2a}^{+\bullet}$ and $\mathbf{2b}^{+\bullet}$ are distinguished by a broad band in the NIR. In the case of $\mathbf{2a}^{+\bullet}$, wavelength-selective photolyses reveal the presence of *two* interconvertible species with very similar yet distinct spectra. Based on DFT and CASSCF/CASPT2 calculations, we assign these spectra to two "electromeric" forms of $\mathbf{2a}^{+\bullet}$ which differ in the nature of the singly occupied MO and in the dihedral angle between the two allyl moieties (all bond lengths and bond angles being otherwise very similar).

Calculations predict that similar electromers should also exist in $\mathbf{2b}^{+\bullet}$, but no corresponding experimental evidence could be found. On the other hand, the ESR spectra indicate that, in contrast to $\mathbf{2a}^{+\bullet}$, the spin appears to be largely localized in one of the two allylic moieties in $\mathbf{2b}^{+\bullet}$.

Although no theoretical method is presently available that would allow an accurate modeling of the opposing factors favoring localized or delocalized structures in molecules such as $\mathbf{2a}^{+\bullet}$ and $\mathbf{2a}^{+\bullet}$, the observed trends can be rationalized satisfactorily on the basis of semiquantitative considerations. In particular, the important role of vibronic coupling in shaping the potential surfaces for such systems is highlighted.

Methods

Experimental. Bicyclopropylidenes **1a** and **1b** were synthesized according to previously published procedures.[5,27,28] **1a** was sufficiently volatile to be premixed with the electron scavenger, CH_2Cl_2, and high-purity Ar in a ratio of 1:1:1000. **1b** was introduced into a U-tube placed before the inlet system of a closed-cycle cryostat where it was entrained at a temperature of ca. 0 °C by a stream of Ar containing 1% of CH_2Cl_2 (matrices formed in this way are usually free of aggregates). After deposition of the mixture on a CsI window kept at 20 K, the sample was cooled to 10 K and exposed for 90 min to the output of an X-ray source containing a tungsten target.[29] For the ESR experiments, **1b** was dissolved to a concentration of ca. 1 mol % in $CFCl_3$ and exposed to ca. 0.5 MRad of ^{60}Co γ-irradiation at 77 K. The ESR spectra were recorded on an E9 spectrometer in the range 77−140 K.

Computational. The results presented in Figures 4 and 5 and Tables 1 and 3 were obtained with the B3LYP combination of exchange and correlation functionals[30,31] which has proven to be quite reliable in studies of radical cations in which it was benchmarked against high-level coupled cluster calculations[20,32−34] or in numerous applications where it was used to explain experimental data.[35−41] Its major drawback in studies of radical ions such as $\mathbf{2}^{+\bullet}$, where spin and charge may be fully delocalized or localized in one half of the molecule, is that it artifactually overstabilizes delocalized structures,[18] because of incomplete cancellation of the self-interaction energy of the unpaired electron by current exchange functionals.[17] Due to this artifact, one cannot apply current DFT methodology to study the electronic structure of such compounds. As an accurate account of the subtle balance of forces that favor localization or delocalization requires proper account for dynamic electron correlation, Hartree−Fock SCF methods are also unsuitable to address this problem (in addition, these methods are prone to artifactual symmetry breaking). Accounting for electron correlation by perturbative methods is also impossible, because a localized HF wave function represents such a poor zero-order approximation to a correlated delocalized wave function (or vice versa) that perturbation theory is bound to fail in such cases. For the above reasons, we have purposely refrained from addressing the question of localized versus delocalized states in $\mathbf{2}^{+\bullet}$ by computational means. All DFT calculations were carried out with the Gaussian 98 suite of programs.[42]

The excited-state calculations, of which the results are presented in Table 2, were carried out by the CASSCF/CASPT2 method.[43] The active space contained 11 electrons in 12 orbitals, and in the CASPT2 calculation, all excited states were described to >70% by the CASSCF wave function. We used the ANO-S basis set of Pierloot et al.[44] and carried out all calculations with the MOLCAS suite of programs.[45]

Acknowledgment. We thank Dr. Xue-Zhi Qin for recording the ESR spectrum of ionized **1b**. This work was supported by the Swiss National Science Foundation (Project No. 2000-067881.02), the Fonds der Chemischen Industrie, and the Hermann Schlosser Foundation (graduate student stipend for M.v.S.).

Supporting Information Available: (a) Figure showing the IR spectra for the ionization and bleaching of **1a** and schemes representing the results of UHF calculations for $\mathbf{2a}^{+\bullet}$ and $\mathbf{2b}^{+\bullet}$ (pdf file). (b) Tables of Cartesian coordinates and energies of all species discussed in the paper (text file). This material is available free of charge via the Internet at http://pubs.acs.org.

JA037252V

(27) De Meijere, A.; Kozhushkov, S. I.; Späth, T.; Zefirov, N. S. *J. Org. Chem.* **1993**, *58*, 2.
(28) De Meijere, A.; Kozhushkov, S. I.; Späth, T. *Org. Synth.* **2000**, *78*, 142.
(29) Bally, T. In *Radical Ionic Systems*; Lund, A., Shiotani, M., Eds.; Kluwer Academic Publishers: Dordrecht, Germany, 1991; pp 19−20.
(30) Becke, A. D. *J. Chem. Phys.* **1993**, *98*, 5648.
(31) Lee, C.; Yang, W.; Parr, R. G. *Phys. Rev. B* **1988**, *37*, 785.
(32) Hrouda, V.; Bally, T.; Carsky, P.; Jungwirth, P. *J. Phys. Chem. A* **1997**, *101*, 3918.
(33) Hrouda, V.; Roeselova, M.; Bally, T. *J. Phys. Chem. A* **1997**, *101*, 3925.
(34) Hrouda, V.; Carsky, P.; Ingr, M.; Chval, Z.; Sastry, G. N.; Bally, T. *J. Phys. Chem. A* **1998**, *102*, 9297.
(35) Truttmann, L.; Asmis, K. R.; Bally, T. *J. Phys. Chem.* **1995**, *99*, 17844.
(36) Bally, T.; Carra, C.; Matzinger, S.; Truttmann, L.; Gerson, F.; Schmidlin, R.; Platz, M. S.; Admasu, A. *J. Am. Chem. Soc.* **1999**, *121*, 7011.
(37) Bally, T.; Bernhard, S.; Matzinger, S.; Truttmann, L.; Zhu, Z.; Roulin, J.-L.; Marcinek, A.; Gebicki, J.; Williams, F.; Chen, G.-F.; Roth, H. D.; Herbertz, T. *Chem.—Eur. J.* **2000**, *6*, 849.
(38) Bally, T.; Bernhard, S.; Matzinger, S.; Roulin, J.-L.; Sastry, G. N.; Truttmann, L.; Zhu, Z.; Marcinek, A.; Adamus, J.; Kaminski, R.; Gebicki, J.; Williams, F.; Chen, G.-F.; Fülscher, M. *Chem.—Eur. J.* **2000**, *6*, 858.
(39) Schroeter, K.; Schröder, D.; Schwarz, H.; Reddy, G. D.; Wiest, O.; Carra, C.; Bally, T. *Chem.—Eur. J.* **2000**, *6*, 4422.
(40) Bednarek, P.; Zhu, Z.; Bally, T.; Filipiak, T.; Marcinek, A.; Gebicki, J. *J. Am. Chem. Soc.* **2001**, *123*, 2377.
(41) Haselbach, E.; Allan, M.; Bally, T.; Bednarek, P.; Sergenton, A.-C.; de Meijere, A.; Kozhushkov, S.; Piacenza, M.; Grimme, S. *Helv. Chim. Acta* **2001**, *84*, 1670.
(42) Frisch, M. J.; Trucks, G. W.; Schlegel, H. B.; Scuseria, G. E.; Robb, M. A.; Cheeseman, J. R.; Zakrzewski, V. G.; Montgomery, J. A.; Stratmann, R. E.; Burant, J. C.; Dapprich, S.; Millam, J. M.; Daniels, A. D.; Kudin, K. N.; Strain, M. C.; Farkas, O.; Tomasi, J.; Barone, V.; Cossi, M.; Cammi, R.; Mennucci, B.; Pommelli, C.; Adamo, C.; Clifford, S.; Ochterski, J.; Petersson, G. A.; Ayala, P. Y.; Cui, Q.; Morokuma, K.; Malick, D. K.; Rabuck, A. D.; Raghavachari, K.; Foresman, J. B.; Cioslowski, J.; Ortiz, J. V.; Stefanov, B. B.; Liu, G.; Liashenko, A.; Piskorz, P.; Komaromi, I.; Gomperts, R.; Martin, R. L.; Fox, D. J.; Keith, T.; Al-Laham, M. A.; Peng, C. Y.; Nanayakkara, A.; Challacombe, M.; Gill, P. M. W.; Johnson, B. G.; Chen, W.; Wong, M. W.; Andres, J. L.; Gonzales, C.; Head-Gordon, M.; Repogle, E. S.; Pople, J. A. *Gaussian 98*, rev. A1: Gaussian, Inc.: Pittsburgh, PA, 1998.
(43) Andersson, K.; Roos, B. O. *Modern Electronic Structure Theory*; World Scientific Publishing Company: Singapore, 1995; Vol. Part 1, Vol. 2; p 55.
(44) Pierloot, K.; Dumez, B.; Widmark, P.-O.; Roos, B. O. *Theor. Chim. Acta* **1995**, *90*, 87.
(45) Andersson, K.; Blomberg, M. R. A.; Fülscher, M. P.; Kellö, V.; Lindh, R.; Malmqvist, P.-Å.; Noga, J.; Olson, J.; Roos, B. O.; Sadlej, A.; Siegbahn, P. E. M.; Urban, M.; Widmark, P.-O. *MOLCAS*, version 4: University of Lund, Sweden, 1998.